Dielectric function and plasmons in graphene

A. Hill, S. A. Mikhailov and K. Ziegler

Institut für Physik, Universität Augsburg - D-86135 Augsburg, Germany, EU

PACS 73.20.Mf – Collective excitations (including excitons, polarons, plasmons and other charge-density excitations)

Abstract – The electromagnetic response of graphene and the spectrum of collective plasmon excitations are studied as a function of wave vector and frequency. Our calculation is based on the tight-binding band structure, including both valleys. As a result, near the Dirac points we find plasmons whose dispersion is similar to that obtained in the single-valley approximation by Dirac fermions with some anisotropy though. In contrast to the calculation for a single Dirac cone, we find a stronger damping of the plasmon modes due to interband absorption. Our calculation also reveals effects due to deviations from the linear Dirac spectrum as we increase the Fermi energy, indicating an anisotropic behavior with respect to the wave vector of the external electromagnetic field.

Introduction. – Graphene, a single layer of carbon atoms arranged as a honeycomb lattice, is a semimetal with remarkable transport properties [1–4]. This is due to the band structure [5] of the material which consists of two bands which touch each other at two nodes. The electronic spectrum around these two nodes is linear and can be approximated by Dirac cones [1]. Many unusal transport properties are controlled by the fact that the Fermi energy is at the nodes, where the density of states vanishes. However, graphene has been gated such that the Fermi energy can be freely tuned. This has opened a wide field for experiments [6]. In the following we will discuss collective excitation of the 2D electron gas in graphene, caused by an external electromagnetic field. Although this is a standard problem in semiconductor physics, it was studied in the case of graphene only in the Dirac approximation around the nodes [7–11].

We consider an electron gas which is subject to an external potential $V_i(\mathbf{q},\omega)$. The response of the electron gas is a screening potential $V_s(\mathbf{q},\omega)$ which is caused by the rearrangement of the electrons due to the external potential. Therefore, the total potential, acting on the electrons, is

$$V(\mathbf{q},\omega) = V_i(\mathbf{q},\omega) + V_s(\mathbf{q},\omega). \tag{1}$$

V_s can be evaluated self-consistently [12] and is expressed via the dielectric function $\epsilon(\mathbf{q},\omega)$. Then the total potential reads [13]

$$V(\mathbf{q},\omega) = \frac{1}{\epsilon(\mathbf{q},\omega)} V_i(\mathbf{q},\omega). \tag{2}$$

The dielectric function is determined by the specific Hamiltonian of the electron gas. In the present case this is the tight-binding Hamiltonian on a honeycomb lattice.

The aim of our study is to compare the dielectric function of the full honeycomb lattice with previous studies of the single Dirac cone. In contrast to the latter, we can not rely on a closed expression for the integrals but have to integrate over the Brillouin zone numerically.

Model. – Using the tight-binding approximation, (quasi-)electrons in graphene are described by the Hamiltonian [14]

$$H = h_1\sigma_1 + h_2\sigma_2 \tag{3}$$

with Fourier components

$$h_1 = -t\sum_{j=1}^{3}\cos(\mathbf{b}_j\cdot\mathbf{k}), \quad h_2 = -t\sum_{j=1}^{3}\sin(\mathbf{b}_j\cdot\mathbf{k}). \tag{4}$$

$\sigma_{1,2}$ are the Pauli matrices and $\mathbf{b}_{1,2,3}$ are the nearest-neighbor vectors on the honeycomb lattice:

$$\begin{aligned}\mathbf{b}_1 &= d(\sqrt{3}/6, 1),\\ \mathbf{b}_2 &= d(\sqrt{3}/6, -1),\\ \mathbf{b}_3 &= d(-1/\sqrt{3}, 0),\end{aligned} \tag{5}$$

t is the hopping parameter ($\approx$2.8 eV) and d is the lattice constant ($\approx$1.42 Å). The Hamiltonian H satisfies the eigenvalue equation $H|\mathbf{k}l\rangle = E_{\mathbf{k}l}|\mathbf{k}l\rangle$ with eigenvalues $E_{\mathbf{k}l} = (-1)^l E_{\mathbf{k}}$ and the positive square root

$$\chi(\mathbf{q},\omega)=\lim_{\delta\to 0}\sum\int_{BZ}\frac{1}{4}|\kappa^*_{\mathbf{k}}\kappa_{\mathbf{k}+\mathbf{q}}+s|^2\left(\frac{f(E_{\mathbf{k}})-f(-E_{\mathbf{k}})}{E_{\mathbf{k}}-sE_{\mathbf{k}+\mathbf{q}}+\omega-i\delta}+\frac{f(E_{\mathbf{k}})-f(-E_{\mathbf{k}})}{E_{\mathbf{k}}-sE_{\mathbf{k}+\mathbf{q}}-\omega+i\delta}\right)\frac{\mathrm{d}^2k}{\Omega_{BZ}},\tag{8}$$

$E_{\mathbf{k}}=\sqrt{h_1^2+h_2^2}$. Thus, the index l refers either to the conduction band ($l=2$) or to the valence band ($l=1$).

Dielectric function. – The dielectric function can be calculated from the Lindhard formula. Assuming that the wavelength of the electromagnetic wave is much larger than the lattice spacing, the longitudinal component reads [12]

$$\epsilon(\mathbf{q},\omega)=1-\frac{2\pi e^2}{q}\chi(\mathbf{q},\omega),\tag{6}$$

where

$$\chi(\mathbf{q},\omega)=\lim_{\delta\to 0}\sum_{\mathbf{k}ll'}\frac{f(E_{\mathbf{k},l})-f(E_{\mathbf{k}'l'})}{E_{\mathbf{k}l}-E_{\mathbf{k}'l'}+\hbar\omega+i\hbar\delta}|\langle\mathbf{k}'l'|e^{i\mathbf{q}\cdot r}|\mathbf{k}l\rangle|^2\tag{7}$$

with $\mathbf{k}'=\mathbf{k}+\mathbf{q}$. $f(E)=1/(e^{\beta(E-\mu)}+1)$ is the Fermi-Dirac distribution function at inverse temperature $\beta=1/k_BT$ with chemical potential μ. In order to determine $\chi(\mathbf{q},\omega)$ we obtain, after some straightforward calculations for eq. (7), an expression for the polarizability ($\hbar=1$) as

see eq. (8) *above*

where $\kappa_{\mathbf{k}}=(h_1-ih_2)/E_{\mathbf{k}}$. Ω_{BZ} is the area of the two-dimensional Brillouin zone $\Omega_{BZ}=\int_{BZ}\mathrm{d}^2k$. The index s describes intraband (for $s=1$) and interband scattering (for $s=-1$). The integral of eq. (8) is evaluated numerically for different values of the chemical potential μ and different directions of the wave vector $\mathbf{q}$, using the limit of zero temperature.

Plasmons. – Poles in ω of the inverse longitudinal dielectric function $1/\epsilon(\mathbf{q},\omega)$ for a given wave vector $\mathbf{q}$ correspond to collective excitations of electrons which are called plasmons. These poles are located either on the real axis or in the complex plane away from the real axis. The latter can be considered as damped plasmons, generated by scattering with individual electrons. An imaginary term can appear in the integral $\chi(\mathbf{q},\omega)$ of eq. (8) if the denominator $E_{\mathbf{k}}-sE_{\mathbf{k}+\mathbf{q}}+\omega$ vanishes inside the Brillouin zone. In other words, if $(\mathbf{q},\omega)$ is inside the band which is produced by the spectrum of the electrons, *i.e.* where an electronic wave vector $\mathbf{k}$ exists that satisfies

$$E_{\mathbf{k}+\mathbf{q}}-sE_{\mathbf{k}}=\omega\qquad(s=\pm1),\tag{9}$$

(cf. fig. 1), scattering between plasmons and electrons is possible and will lead to damping of plasmons. On the other hand, outside the spectrum of electrons (*i.e.*, when there is no electron wave vector k which solves eq. (9)) we obtain undamped plasmons.

As an approximation we can expand the electronic dispersion around the nodes in the $E=0$ plane. This gives

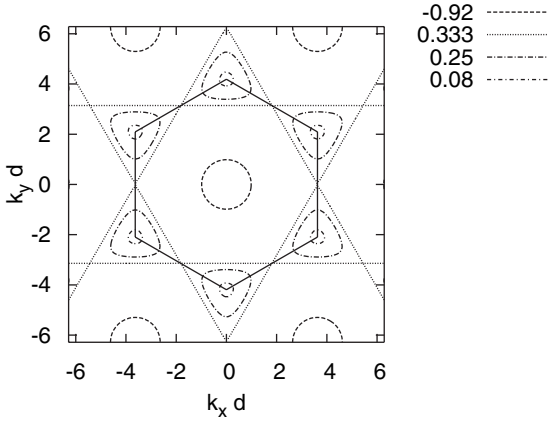

Fig. 1: Contourplot of the electronic dispersion for different energies. The Brillouin zone is indicated by the hexagon which connects the Dirac nodes.

two independent Dirac cones (valleys) with linear dispersion $E_k\sim\gamma k$ around each node. Then the poles of the inverse dielectric function can be evaluated exactly [7, 8]. In this case the plasmon dispersion follows a square root: $\omega_P\sim cq^{1/2}$.

Collective excitations, on the other hand, depend on the spectral properties of the electrons. Therefore, deviations from Dirac cones can affect them. We found that these deviations lead to a stronger damping of the electrons, since electronic excitations require lower energies on the honeycomb lattice in comparison with the linearized (Dirac) spectrum.

In the following we study the imaginary part of the inverse dielectric function [9]

$$Im\left(\frac{1}{\epsilon(\mathbf{q},\omega)}\right)=\frac{-\epsilon''}{\epsilon'^2+\epsilon''^2},\tag{10}$$

where ϵ' (ϵ'') is the real (imaginary) part of the dielectric function itself. Equation (10) is related to the energy loss which can be measured in experiments using high-resolution angle-resolved reflection electron energy loss spectroscopy (HREELS) [15,16]. Our results agree with those experiments for low energies in ref. [15], whereas the high-energy results of ref. [16] are beyond our tight-binding approximation. This quantity becomes a sharp Dirac delta function for a pole of $1/\epsilon(\mathbf{q},\omega)$ on the real axis. If the pole is away from the real axis it becomes a Lorentzian which has a width ϵ'', implying that the width of the Lorentzian is a measure for damping by electron scattering.

Discussion. – The polarizability χ of eq. (8) is evaluated numerically and the corresponding dielectric function

$$\omega_p(q) = \frac{\sqrt{(4a + v_F^2 q)\, q\, (q^4 v_F^4 + 4q^3 v_F^2 a + 16 k_F^2 a^2)}\, \left(v_F^2 q + 2a\right)}{4\,(4a + v_F^2 q)\, a k_F} \tag{11}$$

is obtained from eq. (6) for different values of the frequency ω, the wave vector $\mathbf{q}$ and chemical potential (Fermi energy) μ. All energies are measured in units of the electronic bandwidth ($\Delta = 3t$), and wave vectors are measured in units of the inverse lattice constant.

The electronic dispersion is plotted for several Fermi energies in fig. 1. The contours are Fermi surfaces that indicate at which wave vectors electronic intraband scattering occurs for a given Fermi energy. For $\mu = 0.08$ we have intraband scattering only very close to the Dirac points and the dispersion is Dirac like. In this regime the carrier density can be estimated as [4] $n = k_F^2/\pi \approx 3 \times 10^{13}\,\mathrm{cm}^{-1}$. For $\mu = 0.25$ this gives as a rough approximation $n \approx 1 \times 10^{14}\,\mathrm{cm}^{-1}$. Such high densities may not be available from an external gate but from chemical doping. As we increase μ we see the effect of "warping" and for $\mu = 1/3$ intraband scattering between different valleys is very likely because we have a connected Fermi surface. Finally, for $\mu = -0.92$ we have only a circular Fermi surface around $k = 0$ with parabolic dispersion. This case corresponds with a conventional 2D electron gas.

The plots in fig. 2 show the anisotropy of the plasmon dispersion as a consequence of the band structure of graphene. Remarkable is the strong deviation from the Dirac case for $q_x = q_y$ in fig. 2(c). In fig. 3 it can be seen how the plasmon dispersion changes with the Fermi energy μ. The curvature of $\omega_P(\mathbf{q})$ is negative for low energies (a square-root behavior close to the Dirac points), it increases with μ and becomes positive for energies higher and larger momenta q. This behavior indicates a crossover from the square-root law of Dirac fermions to the behavior of the conventional 2D electron gas [17]

see eq. (11) *above*

with $a = 2ne^2/m$, the effective electron mass m, and the Fermi velocity v_F. Expansion for small q gives

$$\omega_p^2 \approx aq + \frac{3}{4} v_F^2 q^2, \tag{12}$$

which is compared with the findings for graphene at $\mu = -0.92$ (cf. fig. 4). Thus, electrons in graphene behave like in a conventional 2D electron gas. This means that if it is possible to vary the Fermi energy between the linear and the parabolic regime, the behavior of the fermions in graphene could be "switched" from relativistic Dirac fermions to ordinary electrons.

In the theory presented above we have made two approximations. First, we have used the tight-binding approximation, which ignores effects on the atomic scale. Second, using the Lindhard formulas (6), (7) we have ignored the local field effects [18]. Both assumptions restrict the absolute value of the wave vector $\mathbf{q}$ by the conditions $qa_0 \lesssim 1$ and $qd \ll 4\pi/3$, therefore the plasmons spectra are plotted in figs. 2 and 3 at $qd \leqslant 1.5$, which is still within the applicability conditions of the theory.

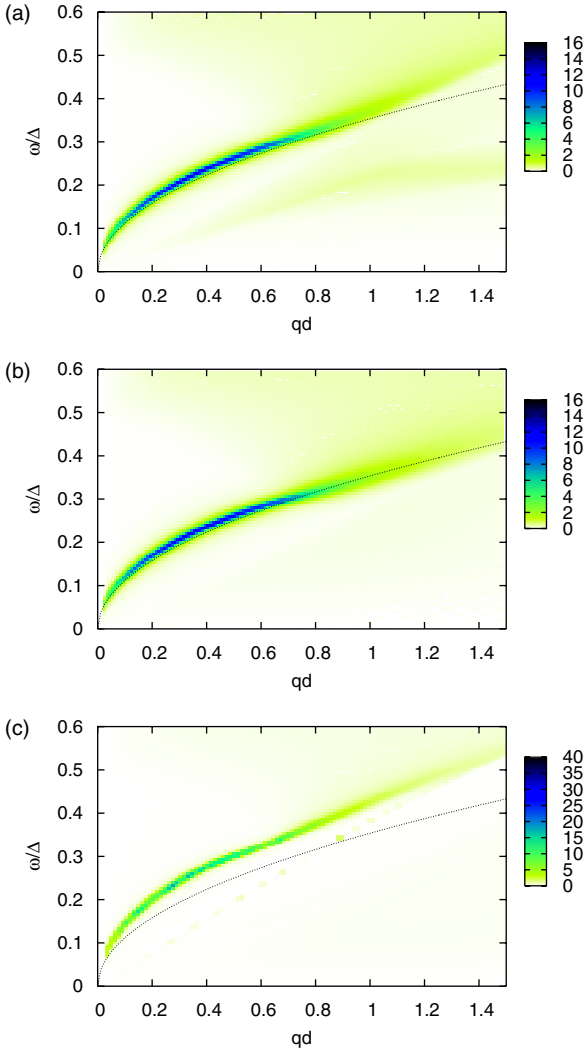

Fig. 2: (Color online) Plasmon dispersion for $\mu = 0.25$ and different directions of the q vector a) $q_x = 0$, b) $q_y = 0$, c) $q_y = q_x$. The square-root behavior of the Dirac case is also shown as a dotted curve.

In fig. 5, however, we also present our results for the plasmon spectrum at larger values of q, up to $qd \simeq 4$. In spite of at so large q the theory is not quantitatively applicable, one can expect that it provides a reasonable qualitative description of the plasmon spectra in graphene. One sees that, while the low-frequency plasmon mode with the frequency $\omega_P \sim \sqrt{q}$ gets a large damping and disappears at $\omega/\Delta \simeq 0.5$, at even higher energies $\omega/\Delta \gtrsim 0.8$ the plasmon mode reappears again. Both plasmon

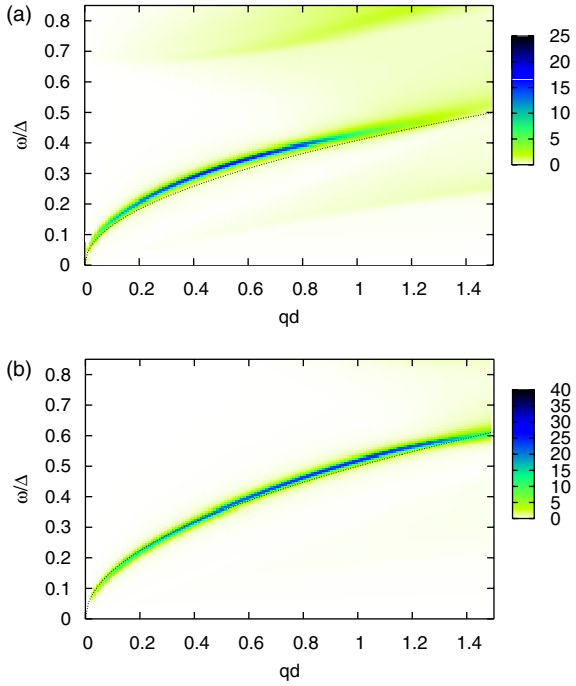

Fig. 3: (Color online) Plasmon dispersion for $q_x = 0$ and different values of the Fermi energy μ. a) $\mu = 0.33$, b) $\mu = 0.5$.

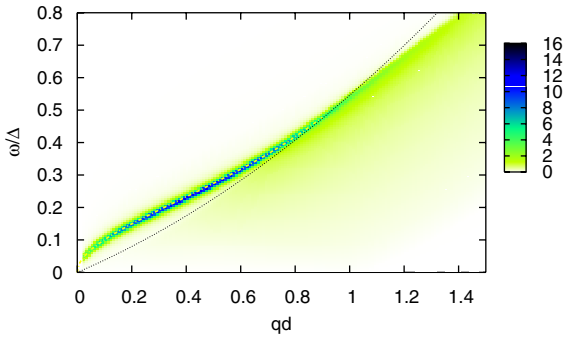

Fig. 4: (Color online) Plasmon dispersion for $q_x = 0$ and $\mu = -0.92$. Here we compare with the conventional (parabolic) 2D electron gas (dash-dotted curve). The curve is the plasmon dispersion of a conventional 2D electron gas of eq. (11), below the dotted line is the intraband single-particle excitation area of a 2D electron gas.

branches look like two parts of the same dispersion curve, "teared" to the low- and high-frequency pieces by the area of the substantial interband damping at $0.5 \lesssim \omega/\Delta \lesssim 0.8$. This interesting result needs to be studied further within a more advanced theory which takes into account the local field effects [18].

Conclusion. – In this paper we have studied the dielectric function of graphene and the plasmon dispersion in tight-binding approximation, and compared the results with similar calculations for a single Dirac cone. There are differences due to the full energy spectrum of the electrons.

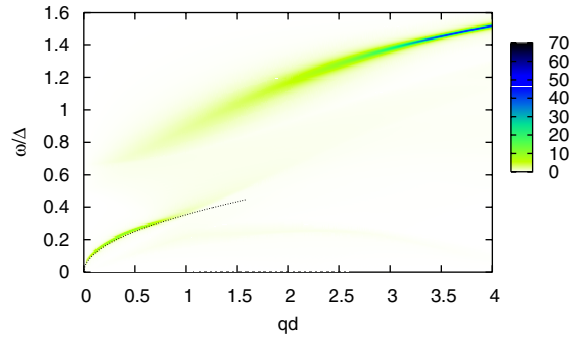

Fig. 5: (Color online) Plasmon dispersion for $\mu = 0.25$ and $q_x = 0$.

It turns out that the damping of the plasmons is stronger, which indicates more scattering between plasmons and single electrons on the honeycomb lattice. Moreover, the plasmon dispersion is not isotropic. Although the dispersion fits well the square-root behavior $\omega_P \sim q^{1/2}$ at small q values, there are substantial deviations for larger values. Finally, a new branch appears in the plasmon dispersion for higher energies ω and larger wave vectors q which needs to be subject of further investigations. Our results reflect a crossover from Dirac-like behavior to conventional electron gas behavior by changing the electron density with the help of a gate.

* * *

We are grateful to T. Tudorovskiy for useful discussions. This work was supported by the Deutsche Forschungsgemeinschaft.

REFERENCES

[1] Novoselov K. S., Geim A. K., Morozov S. V., Jiang D., Zhang Y., Dubonos S. V., Grigorieva I. V. and Firsov A. A., *Science*, **306** (2004) 666.
[2] Novoselov K. S., Geim A. K., Morozov S. V., Jiang D., Katsnelsnon M. I., Grigorieva I. V., Dubonos S. V. and Firsov A. A., *Nature*, **438** (2005) 197.
[3] Zhang Y., Tan Y. W., Stormer H. L. and Kim P., *Nature*, **438** (2005) 201.
[4] Castro Neto A. H., Guinea F., Peres N. M. R., Novoselov K. S. and Geim A. K., *Rev. Mod. Phys.*, **81** (2009) 109.
[5] Semenoff G. W., *Phys. Rev. Lett.*, **53** (1984) 2449.
[6] Geim A. K. and Novoselov K. S., *Nat. Mater.*, **6** (2007) 183.
[7] Wunsch B., Stauber T., Sols F. and Guinea F., *New J. Phys.*, **8** (2006) 318.
[8] Hwang E. H. and Das Sarma S., *Phys. Rev. B*, **75** (2007) 205418.
[9] Polini M., Asgari R., Borghi G., Barlas Y., Pereg-Barnea T. and MacDonald A. H., *Phys. Rev. B.*, **77** (2008) 081411(R).

[10] Shung K. W. K., *Phys. Rev. B*, **34** (1986) 979.
[11] Shung K. W. K., *Phys. Rev. B*, **34** (1986) 1264.
[12] Ehrenreich H. and Cohen M. H., *Phys. Rev.*, **115** (1959) 786.
[13] Mahan G., *Many Particle Physics* (Plenum Press, New York) 1990.
[14] Ziegler K., *Phys. Rev. Lett.*, **97** (2006) 266802.
[15] Liu Yu, Willis R. F., Emtsev K. V. and Seyller Th., *Phys. Rev. B.*, **78** (2008) 201403(R).
[16] Eberlein T., Bangert U., Nair R. R., Jones R., Gass M., Bleloch A. L., Novoselov K. S., Geim A. and Briddon P. R., *Phys. Rev. B.*, **77** (2008) 233406.
[17] Stern F., *Phys. Rev. Lett.*, **18** (1967) 546.
[18] Adler S. L., *Phys. Rev.*, **126** (1962) 413.